

## Melting of Graphite at Very High Pressure

F. P. Bundy

Citation: *J. Chem. Phys.* **38**, 618 (1963); doi: 10.1063/1.1733715

View online: <http://dx.doi.org/10.1063/1.1733715>

View Table of Contents: <http://jcp.aip.org/resource/1/JCPSA6/v38/i3>

Published by the [American Institute of Physics](#).

---

### Additional information on *J. Chem. Phys.*

Journal Homepage: <http://jcp.aip.org/>

Journal Information: [http://jcp.aip.org/about/about\\_the\\_journal](http://jcp.aip.org/about/about_the_journal)

Top downloads: [http://jcp.aip.org/features/most\\_downloaded](http://jcp.aip.org/features/most_downloaded)

Information for Authors: <http://jcp.aip.org/authors>

## ADVERTISEMENT



**ACCELERATE AMBER AND NAMD BY 5X.**  
**TRY IT ON A FREE, REMOTELY-HOSTED CLUSTER.**

[LEARN MORE](#)

## Melting of Graphite at Very High Pressure

F. P. BUNDY

General Electric Research Laboratory, Schenectady, New York

(Received 24 September 1962)

A method of flash-heating small rods of graphite inside a superpressure cell has been developed. The heating energy was inserted in less than 7 msec from a bank of electrolytic capacitors. This quick heating and cooling allowed fusion and freezing of the graphite to occur without serious melting or reaction of the surrounding wall material. Electrical data were recorded with oscillographs and cameras. The start of melting was found to be indicated by an abrupt downward trend of resistance. Polished cross sections of the samples showed clearly the part which melted. Melting temperatures increased from about 4100°K at 9 kbar to a maximum of about 4600°K in the region of 70 kbar, then decreased to about 4100°K at 125 kbar. A value of 25 kcal/mole for the heat of fusion at 48 kbar was determined. The graphite/diamond/liquid triple point is shown to be at about 4000 to 4200°K and 125 to 130 kbar.

### I. INTRODUCTION

THE melting of carbon has been a subject of investigation by scientists for over sixty years. In 1902 Ludwig<sup>1</sup> experimented with the melting of carbon rods by electrical heating in an atmosphere of high-pressure hydrogen. Among the interesting things he observed was that at very high temperatures the electrical resistance of the rod increased abruptly and the heating current was interrupted momentarily. Ludwig thought that this was caused by the formation of liquid, or a nonconducting form of carbon (like diamond), and tried to capture this other form of carbon by rapid quenching. It always came out as graphite.

In 1939 Basset<sup>2</sup> reported an extensive series of experiments in which he heated carbon rods in an atmosphere of high-pressure argon. By use of an optical pyrometer for temperature measurement, and by careful observation of the character of the rod after the experiment to determine whether it melted or was vaporizing, he established the graphite/liquid/vapor triple point to be at about 110 atm and 4000°K. In 1959 Noda<sup>3</sup> reported results of work similar to that of Basset, aimed at determining the triple point and also the crystal lattice parameters of the graphite formed by the freezing of liquid carbon. He concluded that the triple point lies between 110 and 140 atm at a temperature of  $4020 \pm 50^\circ\text{K}$ . The  $c_0$  lattice spacing of the frozen material was found to be 6.709 Å compared to 6.714 Å for the crater material (highly annealed but not melted), and 6.726 Å for the original material. The degrees of crystal perfection of the frozen, the highly annealed, and the original graphites, expressed as the probability of amorphous carbon being present, were 0.03, 0.12, and 0.24, respectively.

Theoretical studies of Pitzer and Clementi,<sup>4</sup> pub-

lished in 1959, suggested that the molecules of liquid carbon should be essentially infinitely long polymeric chains, and that the heat of fusion should be about 10 kcal/mole at 4000°K.

The development of improved high pressure apparatus and techniques in recent years have made it possible to study graphite at very high pressures and temperatures. The goals of the experimental work reported here were to determine the melting point of graphite as a function of pressure, to find the value of the latent heat of fusion, and to locate the triple point for graphite/diamond/liquid. It is believed that all three goals were attained with a fair degree of accuracy.

### II. EXPERIMENTAL

Earlier work at this laboratory by H. T. Hall and by R. H. Wentorf, Jr., indicated that there are no available cell wall materials which are inert enough, and refractory enough, to satisfactorily hold liquid carbon in an ultra-high pressure cell under steady-state conditions. It was found at the beginning of the present work that this difficulty could be overcome by using quick transient heating of the graphite sample by discharge of an electric capacitor through it. The time constants of the electrical circuit could be adjusted so that the graphite sample was heated to the desired temperature and cooled off again before there was appreciable reaction or melting of the wall material. It was also found that adequate electrical measurements could be obtained during the flash-heating by use of a two-channel oscilloscope and camera.

A "belt"-type high-pressure apparatus<sup>5</sup> was used for nearly all the experiments. The arrangement of the test cells most used in the experiments is shown in Fig. 1. The pistons of the pressure apparatus squeezed the cell from above and below while the cylinder part of the apparatus (not shown) confined the periphery. The graphite sample rods were 0.040 in. in diameter and 0.28 in. long. At each end the heating current was spread to much lower current density by the graphite

<sup>1</sup> A. Ludwig, *Z. Elektrochem* **8**, 273 (1902).

<sup>2</sup> M. J. Basset, *J. Phys. Radium* **10**, 217 (1939).

<sup>3</sup> T. Noda, reported by H. Mu, *Proceedings of the International Symposium on High Temperature Technology, Asilomar Conference Grounds, California, October 6-9, 1959: Stanford Research Institute, Menlo Park, California*. (McGraw-Hill Book Company, Inc., New York, 1959).

<sup>4</sup> K. S. Pitzer and E. Clementi, *Science* **129**, 1287 (1959); *J. Am. Chem. Soc.* **81**, 4479 (1959).

<sup>5</sup> H. T. Hall, *Rev. Sci. Instr.* **31**, 125 (1960).

cones and end washers. The heating current entered through one piston, passed directly through the sample, and went out through the other piston. The graphite sample was surrounded by a sleeve of refractory material such as boron nitride, pyrophyllite, MgO, or diamond powder.

Simplified calculations of the rate of temperature decay of the hot graphite rod surrounded by cold boron nitride, based on the ordinary values of thermal conductivity and heat capacity, indicated a half-temperature cool-off time of about 30 msec. The electrical heating circuit was then designed to give 90% energy insertion in a period of 3 to 5 msec. In some of the experiments in which it was desired to follow the cooling behavior of the graphite sample, the circuit was expanded to include a secondary delayed discharge branch, and two more oscilloscopes, as shown in Fig. 2.

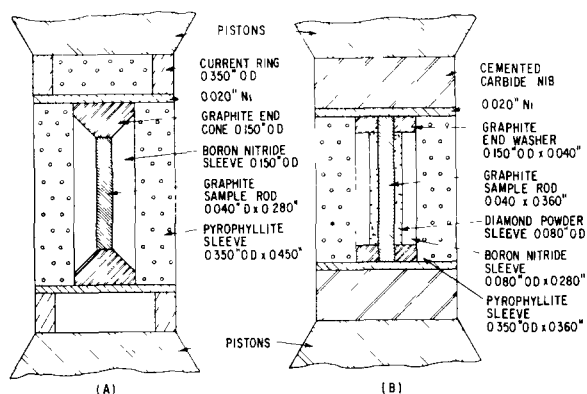


FIG. 1. Test cells used in the graphite melting experiments.

In Fig. 2 the main heating circuit is comprised of the 0.085-F electrolytic capacitor, the switch, the "current resistor"  $R_s$ , the graphite sample, and the 25- $\mu$ H choke coil. The secondary "tailing circuit" consisted of the 0.011-F electrolytic capacitor and 33- $\mu$ H choke in parallel with the main capacitor. The two-channel Tektronix 535A oscilloscopes were connected to the sample and current resistor, as shown, to display simultaneously the voltage drop across the sample, and the current through it. The sweep delays and the sweep rates of the three oscilloscopes were set so that the first oscilloscope registered the first 5 msec and included the main heating pulse. The second responded to the 4- to 14-msec interval, and the third recorded the 10- to 60-msec interval. Three oscilloscopes had to be used because the current and voltage levels to be displayed varied by several orders of magnitude during the 60-msec interval. In most of the experiments the cooling part of the cycle was not studied. In these cases only one oscilloscope was needed to record the main heating pulse.

From the oscillograms, graphs of the electrical power and resistance versus time could be derived.

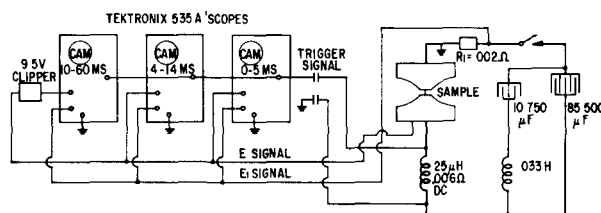


FIG. 2. Circuit used in experiments involving the most complete measurements.

Then the power curve could be graphically integrated to give a curve of inserted energy vs time. Finally the resistance was plotted as a function of the inserted energy. In this way any obvious irregularities in the resistance, which might be a result of phase changes, could be associated with an inserted energy, or temperature.

Figure 3 shows a typical resistance vs time curve for a 100 V flash-heating of a sample of spectroscopic graphite at a pressure of 48 kbar. In this case 70% of the energy had been inserted by 3 msec, and 98% by 7 msec. The curve beyond 7 msec corresponds to cooling off of the sample. The significant characteristic points on this curve—points which are referred to frequently in the remainder of this paper—are  $R_0$ , the initial resistance,  $R_b$ , the resistance break-point where carbon melting began;  $R_{min}$ , the point of maximum amount of melting;  $R_{max}$ , the point at which freezing of liquid carbon was completed; and  $R_f$ , the final resistance of the sample at room temperature but still at pressure. The physical significance of these various points was not known at the beginning of this investigation. A large number of tests had to be run at a range of energy insertions, and the samples examined, before it was realized what phenomena were taking place in the cell. As experience was gained, and reproducibility of the phenomena established, it became possible to interpret the results in a quantitative sense.

### III. BEHAVIOR OF SPECTROSCOPIC ROD GRAPHITE

The resistance curve shown in Fig. 3 corresponded to very energetic heating. When a series of tests was carried out on the same type of sample, using a range

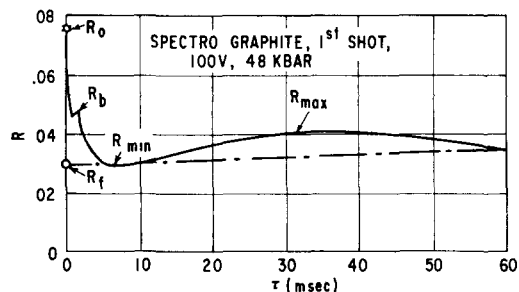


FIG. 3. Resistance-vs-time curve for the initial 100-V flash-heat on spectroscopic rod graphite at 48 kbar.

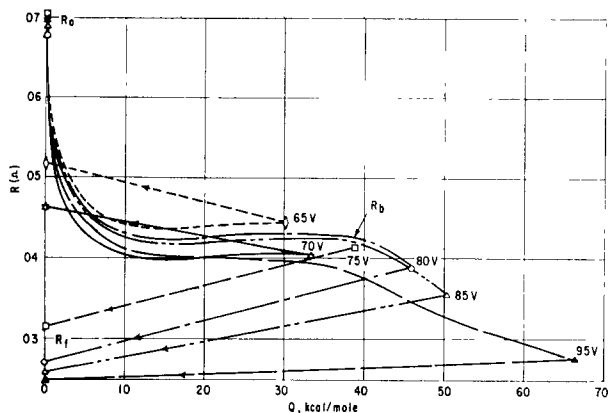


FIG. 4. Family of  $R$ -vs- $Q$  curves for spectroscopic rod graphite in BN sleeves at 48 kbar pressure.

of flash-heating energies that extended from no melting to nearly complete melting, a family of  $R$  vs  $Q$  curves, as shown in Fig. 4, was obtained. Here, the instantaneous resistance is plotted against the energy that had been inserted into the sample up to that instant. Each curve covers the first 5 msec of the flash heat; thus in the 65 V case the sample absorbed 30 kcal/mole in the first 5 msec whereas in the 95 V case it absorbed 66.5 kcal/mole in the same time interval. The straight lines connecting the end of each curve back to zero  $Q$  point to the final  $R_f$  of the sample at room temperature, and are not intended to show the path by which the final resistance was reached. Several characteristics of resistance behavior are evident from this family of curves. First is the rapid drop of resistance which occurred during the insertion of the first 5 to 10 kcal/mole of energy. Second, when the energy exceeded about 38 kcal/mole the resistance inflected downward as melting began. Third, when the total flash-heat energy exceeded the amount required to reach the  $R_b$  point, the final room temperature resistance came to a value less than  $R_b$  whereas for smaller insertion energies  $R_f$  was greater than  $R_b$ .

The latter effect is shown graphically in Fig. 5 where the ratio  $R_f/R_0$  is plotted against the total energy of the flash heat. It is evident from this graph that between about 35 and 42 kcal/mole total energy insertion a radical change took place in the graphite. Further increase in total energy insertion had no effect on the  $R_f/R_0$  ratio. This suggested that 42 kcal/mole heating was sufficient to melt together all the intercrystallite zones in the graphite which had been imperfect electrically conducting regions before.

The series of photomicrographs presented in Fig. 6, taken from polished sections of some of the samples used for the data for Figs. 4 and 5, show the visible structural changes in the graphite. At 32 kcal/mole (65 V) the structure had very nearly the same appearance as the virgin material. At 37 kcal/mole (70 V) a little grain growth was observable, a few of the

crystals showing sharper edges than before. At 75 V (43 kcal/mole) a striking change in the center half (diameter) of the section was evident. In the central zone the crystals were larger and had well-defined edges. At 80 V (49 kcal/mole) the region of strongly modified material was larger, and at the very center there was a trace of a radial crystal structure which developed rapidly as the energy increased. This radial crystal structure, which showed clearly in the higher energy specimens, was a result of very rapid cooling of a completely liquefied core. The dendritic crystals naturally grew from the periphery, where the heat was removed, toward the center. In this case the preferred direction of growth of the graphite was found to be in the  $a$  direction, probably because the thermal conductivity of the graphite crystals is greater in the  $a$  direction than in the  $c$  direction. Those crystals in the unmelted region which happened to be oriented with an  $a$  direction parallel to the radius of the cell could grow faster from the melt than those of other orientations because they could conduct away the latent heat of solidification more rapidly.

The experimental evidence presented in Fig. 4, 5, and 6 indicates that for total energy insertions of less than about 34 to 35 kcal/mole no melting occurs. For energies slightly lower than this some regraphitization and annealing does occur. Between about 38 and 48 kcal/mole melting occurs around crystals and grains, producing a mushy phase which freezes to a randomly oriented mass of large, sharp-edged crystals of nearly ideal electrical conductivity for randomly oriented graphite at the ambient pressure. At about 48 kcal/mole complete melting is attained at the center of the sample. For higher heating energies larger diameter cores of liquid carbon are formed. The electrical resistivity of the liquid carbon is less than that of the solid at the same temperature.

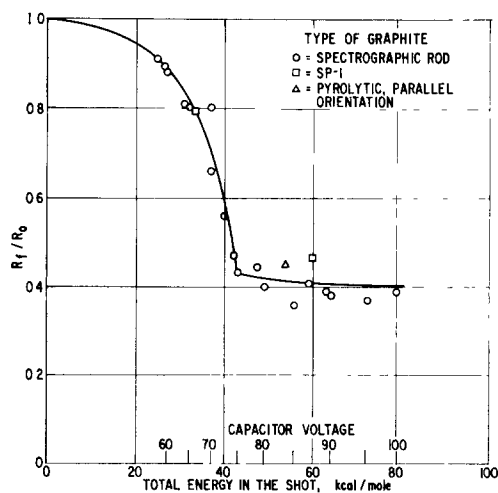


FIG. 5. Ratio of final to initial resistances of graphite samples flash-heated by shots of different total energies at about 50 kbar pressure.

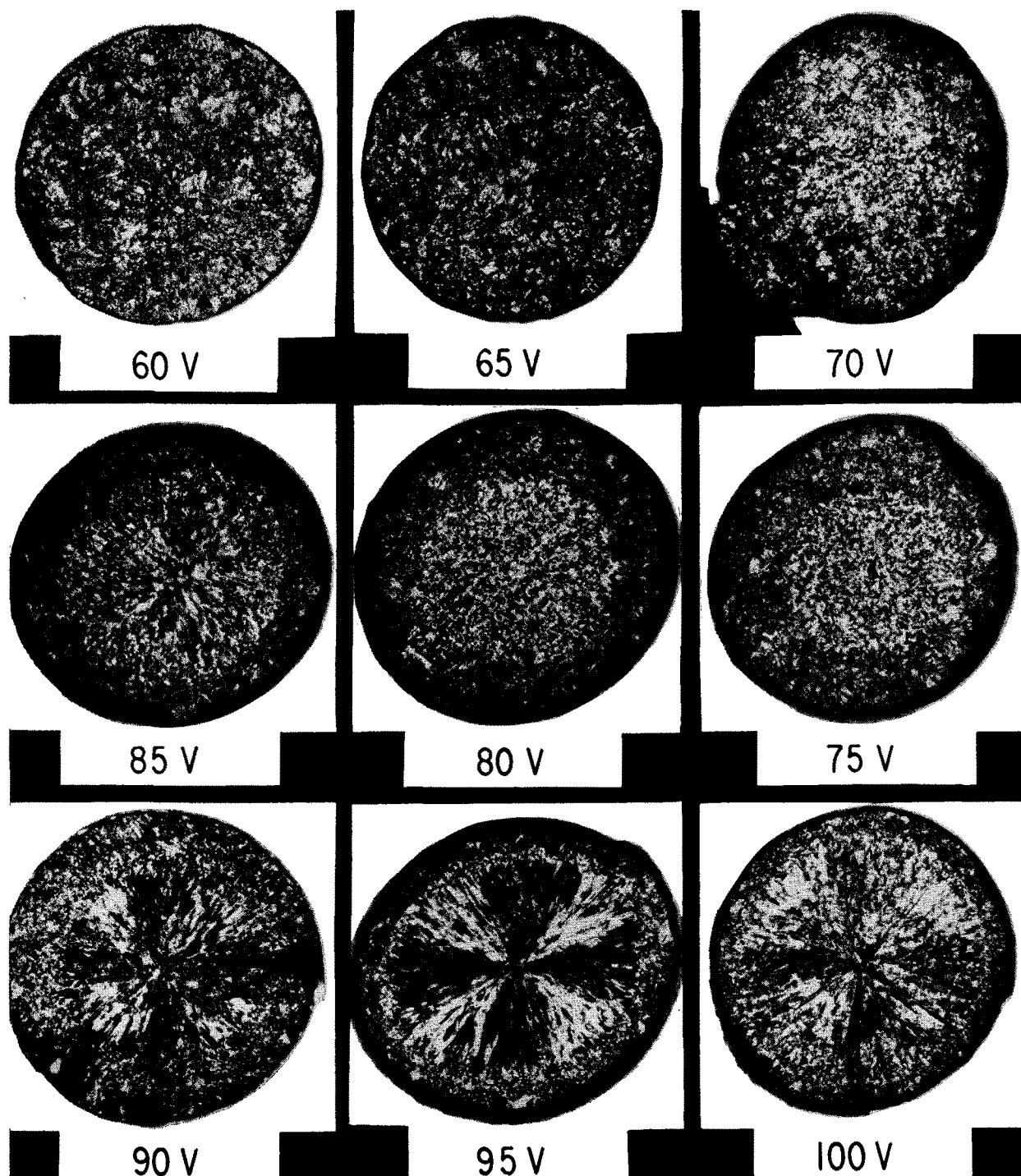


FIG. 6. Series of photomicrographs of polished sections of the graphite samples of Fig. 5 showing the change of character of the graphite structure (48 kbar series).

The  $R_b$  point at which the resistance inflected downward in Fig. 4 is where intergrain melting of the graphite begins. Further addition of heat energy causes more melting by providing the heat of fusion. When a definite core of liquid carbon gets established in the center of the sample this fluid column absorbs a dis-

proportionate fraction of the additional inserted energy because of its lower resistance relative to the surrounding solid graphite which is in parallel electrically. This effect causes the radial temperature gradient to become progressively larger, and in a practical sense makes it difficult to melt the graphite fully to the

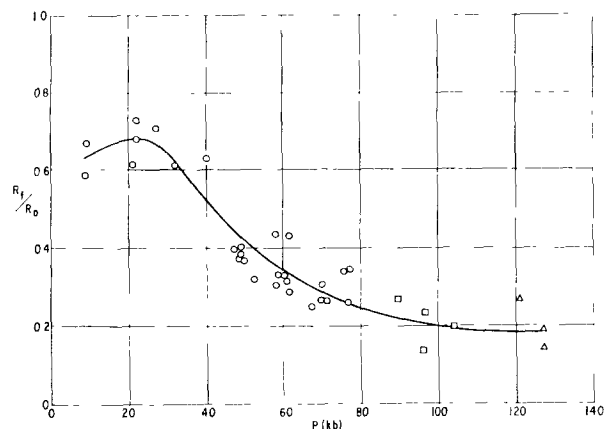


FIG. 7. Ratio of final to initial resistance as a function of the pressure at which the flash heating was done. The energy of the heating flashes ranged from 46 to 108 kcal/mole.

periphery. This same effect makes it difficult to determine analytically from the portion of the  $R$  curve between  $R_b$  and  $R_{min}$  in Fig. 3 how much of the decrease in  $R$  is caused by transformation of solid to liquid, and how much to the increased temperature (superheat) of the liquid core already formed.

The data in Fig. 5 show that the value of  $R_f/R_0$  remains practically constant for all energy inputs greater than that required to start melting. The results of experiments at different pressures beyond about 20 kbar have shown that the value of the terminal  $R_f/R_0$  ratio decreases with the pressure at which the process is performed. Experimental data are presented in Fig. 7. The scatter of the points is probably caused by the variety of graphites and cell geometries used, and by the very wide range of flash-heating energies. The resistivity of graphite flash-melted at about 100 kbar pressure is about  $150 \times 10^{-6} \Omega \text{ cm}$ . This is about one-eighth the resistivity of spectroscopic rod graphite at room pressure and temperature.

After a flash heat, when the pressure on the sample was decreased at room temperature, the resistance increased along a path a little below the curve shown in Fig. 7. If the pressure was increased after a flash-heat the resistance was found to increase at first, but a continued increase of pressure would eventually cause a decrease. When the sample was given a second strong flash heat after a change of pressure at room temperature the new final resistance was found to be near the curve of Fig. 7. Apparently the mechanical expansion or compression of the newly frozen graphite disturbed its structure and increased its electrical resistivity, but such changes could be obliterated by remelting it at the new pressure.

After having established that the downward inflection  $R_b$  in the  $R$  vs  $Q$  curve corresponds to the beginning of melting, it became of interest to find how the melting point varies with pressure. A set of data for

spectroscopic rod graphite is shown in Fig. 8. The tests were carried out at pressures ranging from 9 to 97 kbar. A glance at this family of curves shows that pressure does not have a profound effect on the energy-to-melting. Closer inspection indicates a flat maximum of about 35 kcal/mole at 50 to 60 kbar, and a value of about 30 kcal/mole at the lowest and highest pressures. The most striking effect brought out in Fig. 8 is the great pressure effect on the resistance of solid graphite at the melting temperature. At 97 kbar this resistance is only about half its magnitude at 9 kbar. The same effect holds for the liquid state, but to a greater extent. Thus the effect of high pressure is to reduce the resistivity of high-temperature graphite, and of liquid carbon.

The  $R_b$  points from a large number and variety of experiments are plotted on a  $P$  vs  $Q$  chart in Fig. 9. This accumulation of data shows that in the pressure range up to about 60 kbar the energy required to bring graphite to its melting point increases slowly with the pressure. For pressures above about 60 to 70 kbar the trend is reversed to the extent that at 130 kbar the energy-to-melting is less than it is at 10 kbar. Another interesting thing brought out by this array of data is that a difference of about 15% exists between the energy insertion required to melt graphite contained within boron nitride or pyrophyllite walls as compared to diamond powder or MgO walls. It is believed that this difference is caused mainly by greater electrical leakage in the very hot boron nitride or pyrophyllite walls as compared to diamond or MgO. The latter are

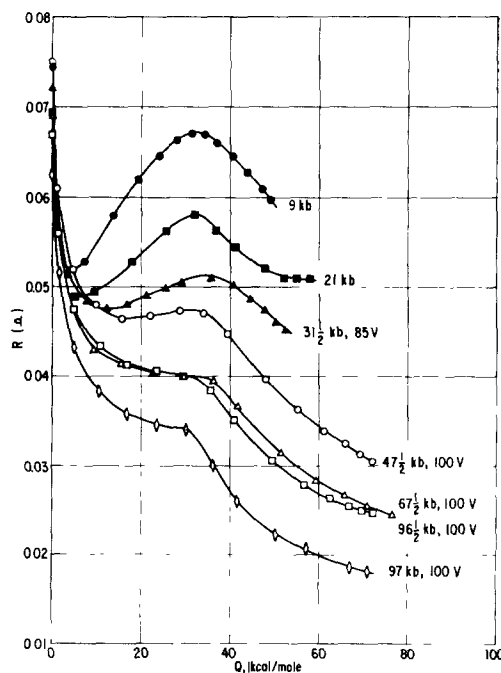


FIG. 8.  $R$ -vs- $Q$  curves for spectroscopic rod graphite in BN sleeves run at different cell pressures.

known to be better electrical insulators at very high temperatures. However, even though diamond and MgO are better than boron nitride and pyrophyllite in this respect, they do allow some loss of energy by thermal conduction and electrical leakage. Therefore one would expect the true curve of energy-to-melting to lie somewhat to the left of the line for diamond walls. Since the thermal and electrical conductivities of these wall materials are not well known at these very high temperatures it was concluded that the best location of the true line would be set by anchoring it at the triple point established by Basset, and by Noda, at 0.1 kbar and 4000 to 4100°K. (See second paragraph of this paper.) Such a line is shown in Fig. 9. This line is used later as a basis to calculate the melting temperature as a function of pressure.

Figure 10 presents a family of  $R$  vs  $t$  curves which show the cool-off behavior of spectroscopic rod graphite in a boron nitride sleeve. The heating shots were made successively on the same sample without lowering the pressure. The shots were made in the order: 100, 75, 80, 85, 90, and 95 V. The curve for the first shot (100 V) is part of the curve shown earlier in Fig. 3. This family of curves exhibits clearly the rise of resistance—which starts at 7 msec—associated with the cooling and freezing of the liquid phase, followed by the decrease of resistance associated with cooling of the solidified graphite. The time interval required for the cooling and solidification of the liquid increases

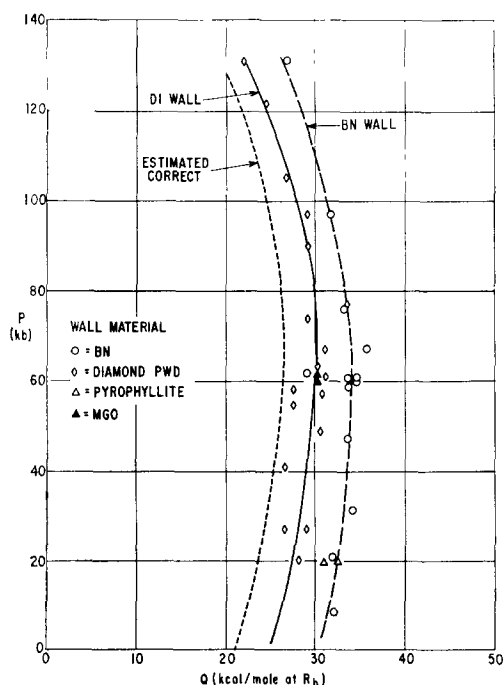


FIG. 9. Summary of data for energy required to reach the melting point at different ambient pressures using a variety of wall materials.

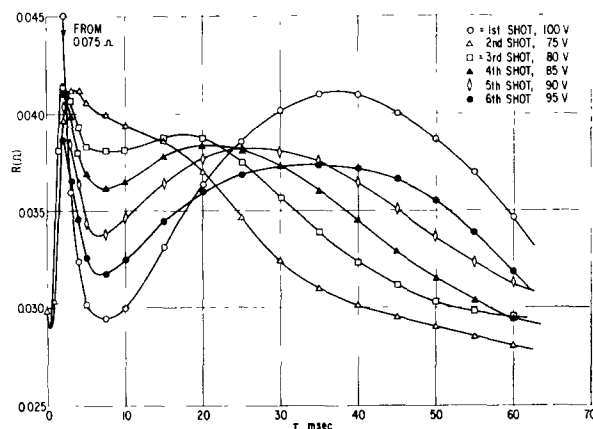


FIG. 10. Family of resistance versus time curves for spectroscopic rod graphite in boron nitride sleeve at 48 kbar pressure.

with the amount and temperature of the liquid formed during the energy injection. The 75-V shot, according to the photomicrograph in Fig. 6, produced only a small amount of liquid phase and consequently yielded only a slight dwell on the resistance-time curve. By contrast, the 100-V shot, which melted almost all the graphite sample, gave a large rise of resistance during the liquid cooling and freezing period. The information contained in this family of curves, together with heating power and specific heat data, is used later in this paper to deduce the heat of fusion of graphite.

The photomicrograph of the 100-V specimen in Fig. 6 indicates that the graphite was almost completely melted. If it were truly melted the resistance of the column of hot liquid carbon formed should be independent of the exact structural and crystal form of the graphite from which it was derived. Therefore a second 100-V shot should bring the sample to the same resistance when at maximum temperature. The curves of  $R$  vs  $Q$  in Fig. 11 show that this is the case. At the beginning of the first shot the virgin sample had a resistance of 0.0715  $\Omega$  and the structure shown in Fig. 6 (60 V), whereas at the start of the second 100 V shot the resistance was 0.0235  $\Omega$  and the structure shown in Fig. 6 (100 V). A second interesting thing brought out in Figs. 10 and 11 is that the graphite formed by freezing of liquid carbon has a positive temperature coefficient of resistance, like a metal. The experiments indicated that this is generally the case for all the randomly oriented polycrystalline graphites tested.

#### IV. BEHAVIOR OF OTHER TYPES OF GRAPHITE

Graphite is available in many different kinds of crystal and structural arrangements. One would suppose, however, that any of the solid forms should melt to the same kind of liquid. In addition to the experiment described in the previous paragraph many other experiments were carried out to test this idea, as well

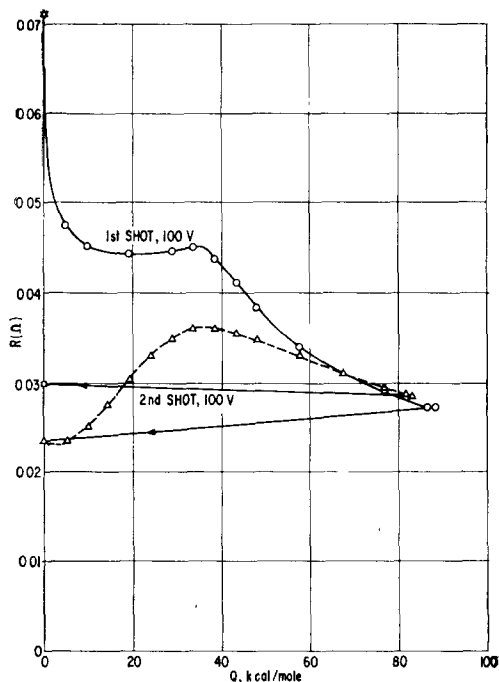


FIG. 11. Resistance behavior of spectro rod graphite in boron nitride sleeve during the first two strong flash heatings. Even though the initial resistances are quite different because of the different structures of the graphite, the  $R_b$  points occur at nearly the same energy insertion, and the hot liquid at 60 to 80 kcal/mole seems to be the same in each case (9.3 mg, 59 kbar).

as to observe any unusual effects that might occur during the heat-up or cool-off processes. Among the graphites tested were: unannealed pyrolytic with the

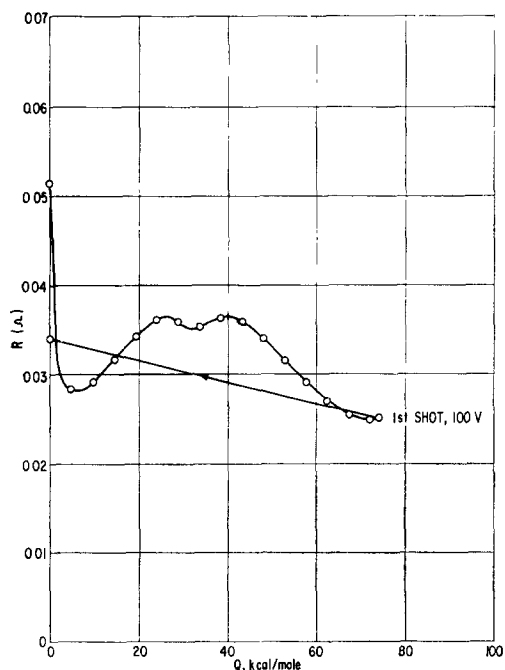


FIG. 12.  $R$ -vs- $Q$  behavior of unannealed "parallel" pyrolytic graphite (12.7 mg, 62 kbar).

crystal planes concentric around the axis of the cell; unannealed pyrolytic with the crystal planes perpendicular to the cell axis; and SP-1 flake graphite (National Carbon Company).

The behavior of unannealed "parallel" pyrolytic graphite is shown in Fig. 12. Its initial resistance was lower than spectroscopic rod graphite, and its resistance dropped to unusually low values during the insertion of the first 5 kcal/mole of energy. From 5 to 25 kcal/mole it increased steadily to a maximum. From 25 to 40 kcal/mole the resistance decreased to a shallow minimum and back to a maximum. At about 40 kcal/mole melting definitely started and continued

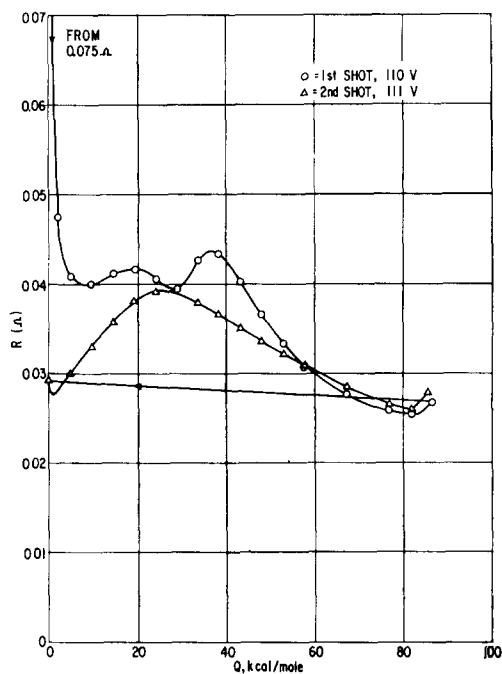


FIG. 13.  $R$ -vs- $Q$  curves for unannealed "concentric" pyrolytic graphite. (11.1 mg, 62 kbar).

in the usual manner to the end of the energy insertion where the resistance came to about the same value as for the liquid formed from spectroscopic graphite. All the runs made with parallel pyrolytic graphite showed this same double maximum in the resistance. Thus this behavior is a reproducible characteristic of this kind of graphite and cell geometry. More experiments and study are necessary to work out a satisfactory explanation of this phenomenon. The most direct explanation is that the temperature coefficient of resistance of graphite crystals in the "a" direction alternates between positive and negative as the temperature increases. Another is that the large asymmetry of thermal conductivity in the azimuthal plane of the cell causes the graphite to reach the melting point at different places in the sample at slightly different times.

The results for the "concentric" pyrolytic graphite are shown in Fig. 13. As in the preceding case of "parallel" pyrolytic graphite, the heating current flowed parallel to the "a" axes of the graphite crystallites in this sample. The first heating shot showed three pulsations or peaks (the first one is submerged in the initial downward sweep of resistance). This behavior was exhibited by each of the three samples tested so it must be a true characteristic of this graphite and geometry. At the high levels of energy insertion the resistance settled down to the usual value for the hot liquefied core. A second energetic heating shot was administered to this sample with about the same result

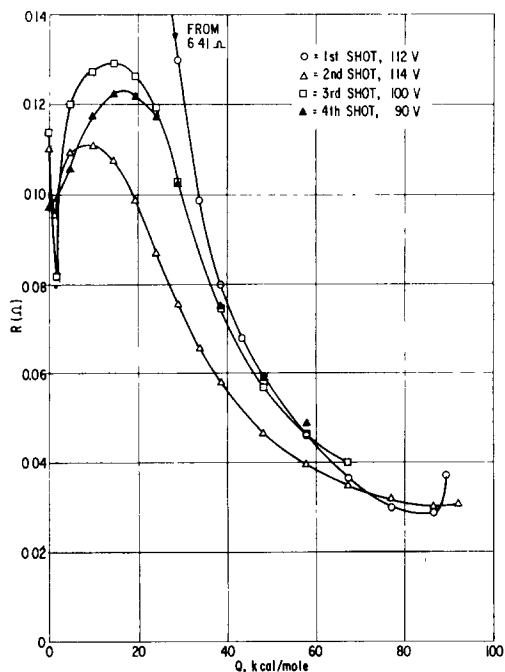


FIG. 14.  $R$  vs  $Q$  for unannealed "perpendicular" pyrolytic graphite (12.2 mg, 62 kbar).

as for the second shot on spectroscopic graphite (Fig. 11). After the shots the cross section of the graphite sample appeared very much like Fig. 6 (100 V), indicating that nearly complete fusion had occurred.

Figure 14 shows the results for several successive heating shots on a sample of unannealed "perpendicular" pyrolytic graphite. This material had a very high initial resistance; 6.4  $\Omega$  compared to 0.05  $\Omega$  for the same material in the parallel orientation. At the highest temperatures this material showed about the same resistivity as the other kinds of graphite, indicating that it melted to about the same extent. The cross sections after the runs showed almost complete radial patterns, like Fig. 6 (100 V), which also indicated nearly complete fusion. The striking difference from the other graphites was that upon freezing and cooling the sample returned to relatively high resistance. This

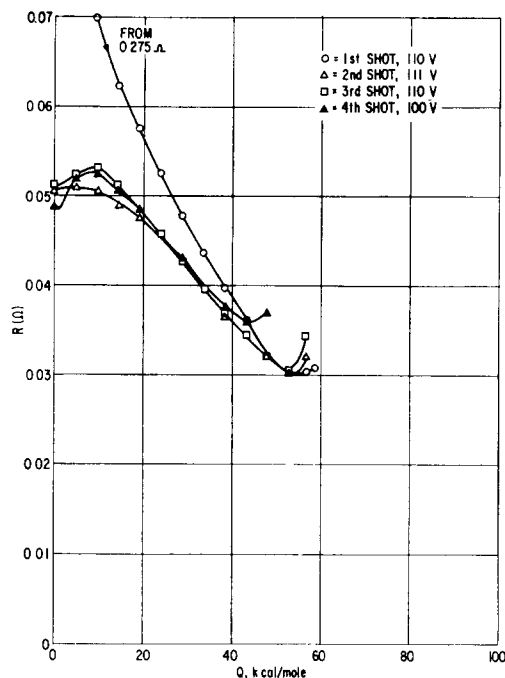


FIG. 15.  $R$  vs  $Q$  for strongly annealed "perpendicular" pyrolytic graphite. (17.5 mg, 62 kbar).

effect was almost certainly caused by the preferred orientation of the unmelted graphite crystallites which remained on the relatively cool walls. These crystallites would naturally grow back in the original "perpendicular" orientation and would give the high electrical resistivity that is characteristic of the "c" direction

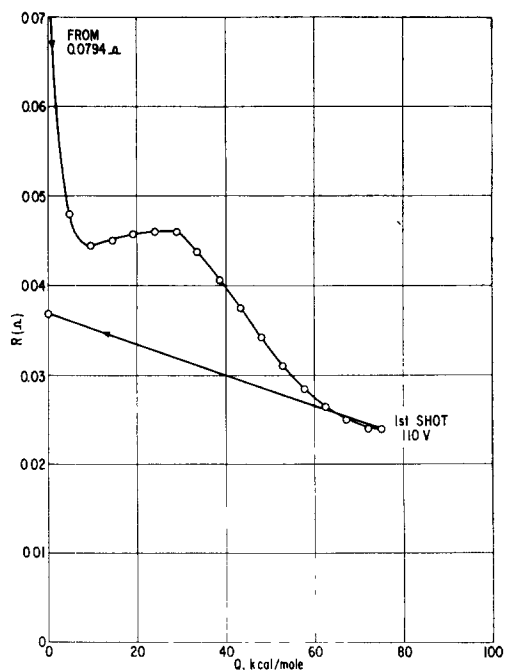


FIG. 16.  $R$ -vs- $Q$  curve for SP-1 graphite (12.5 mg, 62 kbar).

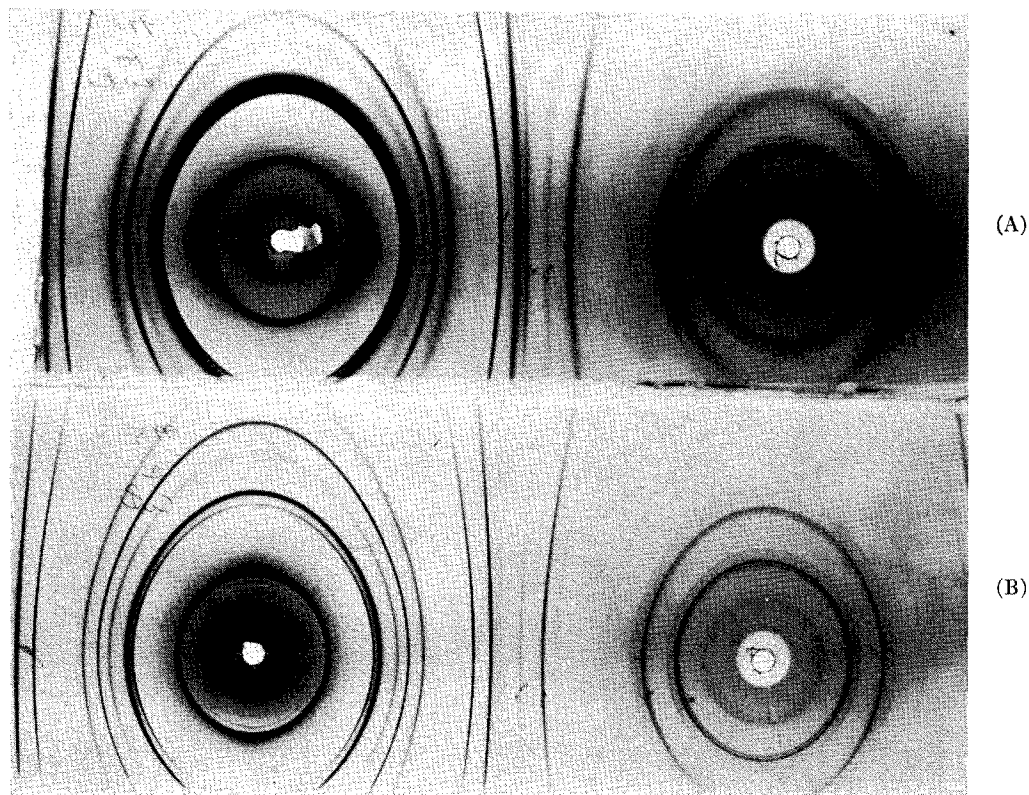


FIG. 17. X-ray diffraction patterns of spectroscopic rod graphite flash heated at 19 kbar. (A) Sample from end of cone (unmelted). (B) Sample from midspan where melting and freezing occurred.

in graphite. The melting and freezing cycle could be carried out many times in succession without losing the characteristic of orientation.

The results for strongly annealed "perpendicular" pyrolytic graphite are shown in Fig. 15. This sample was larger in diameter than standard to the extent that it weighed almost twice as much as a standard spectroscopic rod sample. At maximum safe charging voltage the capacitor was capable of delivering only about 50 kcal/mole to this sample, making extensive melting impossible. However, it can be seen from the trend of the curves that the resistivity would have gone to values comparable to the other kinds of graphites for energy insertions of 80 to 90 kcal/mole. Note that there is great similarity in the curves for the two "c"-axis graphites shown in Figs. 14 and 15.

SP-1 graphite (a very high-purity flake graphite with excellent packing characteristic, made by the National Carbon Company) gave the results shown in Fig. 16. These samples were formed by packing the powder in the bore of the boron nitride sleeves. Because of the flake structure of the powder the packing operation automatically produced a partial "c"-axis orientation. The density of the packed powder approached that of ideal graphite. Figure 16 shows that the insertion of 75 kcal/mole melted the sample and brought it to the same resistivity as spectroscopic

graphite. The relatively high final resistance at room temperature is believed to be a result of the partial "c"-axis orientation of the residual unmelted graphite crystallites on the wall—as in the case of the "perpendicular" pyrolytic graphite samples described above.

Considering all the  $R$  vs  $Q$  data presented in Figs. 11-16 it appears quite certain that the different kinds of graphite do melt to the same kind of liquid, but that there are striking differences in how the liquid state was attained, and that there were definite crystal orientation effects during the freezing process which were controlled by the orientation of the unfused graphite crystallites which remained on the cool wall.

#### V. X-RAY DIFFRACTION PATTERNS

Since the graphite formed by rapid freezing under high pressure offered the possibility of something novel in crystal lattice structure, several x-ray diffraction patterns of the material were made. Figure 17 shows x-ray diffraction patterns of the graphite from two different sites in a sample of spectroscopic rod graphite flash melted at 19 kbar. Pattern (A) was obtained from graphite from one end-cone which was at pressure but did not get very hot. Pattern (B) was obtained from graphite from the center of the rod where melting and freezing had occurred. The locations of the diffraction rings in the two patterns are very nearly identical,

which indicates that the crystal lattice spacings in the two samples are practically the same. However, the diffraction lines from the material which had been melted and solidified are much sharper than those from the unmodified material, showing that the organized crystallite size of the frozen graphite is much larger than that of the unmodified material. The  $c_0$  lattice spacings for patterns (A) and (B) were  $6.746 \pm 0.003 \text{ \AA}$  and  $6.749 \pm 0.001 \text{ \AA}$ , respectively. A different sample, melted at a pressure of 78 kbar, yielded a sharp x-ray diffraction pattern which gave a  $c_0$  spacing of  $6.7415 \pm 0.0001 \text{ \AA}$ .<sup>6</sup> These values are to be compared with those of Noda,<sup>3</sup> mentioned earlier, of  $6.726 \text{ \AA}$  for untreated material and  $6.709 \text{ \AA}$  for melted material. The author has no satisfactory explanation of the differences between the values of Noda and the ones obtained in the present work. One can suspect that the high-pressure argon in Noda's case, or the decompression in the present case, might affect the lattice stacking of the graphite.

Each of the x-ray diffraction patterns was examined for presence of lines of rhombohedral graphite, and of boron nitride. In about half the cases very slight traces of both these materials were detected. It is believed that traces of rhombohedral graphite were formed by shearing of the extremely soft frozen graphite while digging out the sample material with a sharp needle. The traces of boron nitride were found only in those samples which had been flash heated at the highest energies. Resistance evidence indicated that the small contamination that did occur, took place late in the heating period and therefore had no effect on the

primary phenomena during the main part of the heating.

## VI. MELTING TEMPERATURES

In the foregoing presentation the "phenomena points" of graphite have been related to the inserted heating energy. The temperature  $T$  corresponding to a given energy insertion  $Q$  is given by the relation

$$Q = \int_{T_0}^T C_p(T) dT. \quad (1)$$

The specific heat  $C_p$  probably varies some with pressure as well as temperature, but as the variation is probably small, and is unknown, it will not be taken into account. At atmospheric pressure the specific heat of graphite increases from 2.05 cal/mole deg at 300°K to 5.75 cal/mole deg at 1500°K.<sup>7-9</sup> Theoretically, if no additional degrees of freedom of the atoms in the crystal lattice become energized, the specific heat should level out at 6 cal/mole deg at higher temperatures. Hove,<sup>9</sup> who made experimental measurements up to nearly 4000°K found this to be approximately the case up to about 3500°K, but above this temperature his measured values increased very rapidly with temperature as shown in Fig. 18. Hove had serious experimental difficulties at temperatures above 3400°K which had the effect of spuriously increasing the indicated values of specific heat. Thus, although his experimental data were reproducible, they may have been in error on the high side. After discussing this question of specific heat with D. Turnbull, with R. Alpher, and with H. Brooks, at different times, it was concluded that prior to reaching vaporization, or melting, the specific heat of graphite probably increases about linearly with temperature, as Hove found it to do between 1800° and 3200°K. This extrapolation of  $C_p(T)$  was then used in Eq. (1) to establish the  $T$  vs  $Q$  curve shown in Fig. 18. This  $T(Q)$  curve is the one used to transform the  $Q$  values of the present experiments to temperature data.

When the dashed line of Fig. 9 is transformed to  $T$  vs  $P$  by means of the  $T$  vs  $Q$  curve of Fig. 18 one gets the graphite melting line shown in Fig. 19. This shows that graphite has a maximum melting temperature of about 4600°K in the region of 60 to 70 kbar pressure. Increase of pressure beyond this point causes the melting point to decrease until the triple point is reached. The location of the triple point shown in Fig. 19 is based upon a combination of the results of the present

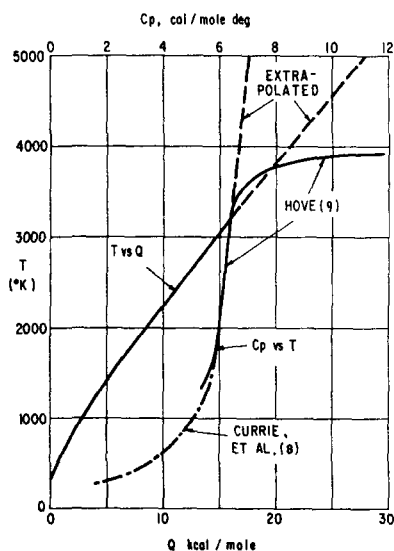


FIG. 18. Curves of  $C_p$  vs  $T$  and  $T$  vs  $Q$  used in this paper.

<sup>6</sup> General Electric XRD apparatus; 50 mm radius camera; Cu  $K\alpha$  radiation; least-square fit to Nelson-Riley extrapolation.  $\pm 0.0001 \text{ \AA}$  is the standard deviation of the measurements. The absolute accuracy is  $\pm 0.0005 \text{ \AA}$ .

<sup>7</sup> H. M. Spencer, *Ind. Eng. Chem.* **40**, 2152 (1948).

<sup>8</sup> L. M. Currie, V. C. Hamister, and H. G. MacPherson, "The Production and Properties of Graphite for Reactors," a paper presented at the U. N. Intern. Conf. Peaceful Uses of Atomic Energy, Geneva, Switzerland, August 8-20, 1955. Published by the National Carbon Company.

<sup>9</sup> J. E. Hove, "Some Physical Properties of Graphite as Affected by High Temperature and Irradiation," in *Industrial Carbon and Graphite* (Society of Chemical Industries, London, 1958).

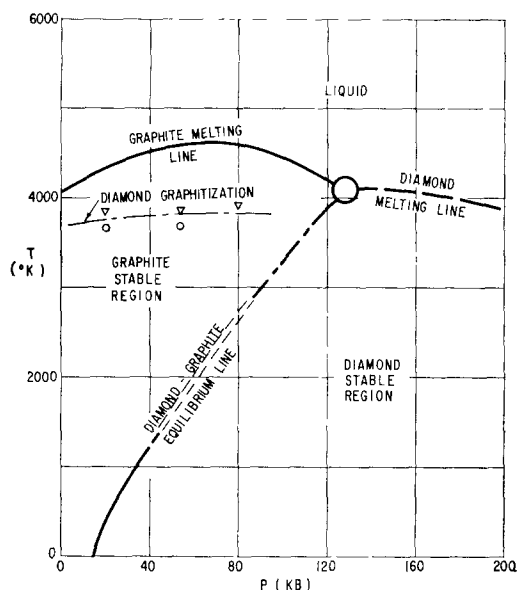


FIG. 19. Melting temperature of graphite as a function of pressure. Also shown are the melting line of diamond, the graphite/diamond equilibrium line, and the graphite/diamond/liquid triple point.

work on graphite melting, the work on the graphite/diamond equilibrium line by catalytic diamond growth and graphitization,<sup>10</sup> and very recent work on the direct transformation of graphite to diamond.<sup>11</sup> This combination of results puts the triple point at about 125–130 kbar pressure and 4000°–4200°K.

Exact points on the diamond melting line have not been obtained experimentally, but the evidence given in reference 11 together with the results of Alder and Christian<sup>12</sup> show quite clearly that the diamond melting line must come into the triple point with a slightly negative slope. Further evidence, obtained in the present work on graphite melting, comes from the behavior of small diamond crystals which were imbedded in some of the graphite rod specimens. It was found experimentally that there was a sharp temperature threshold at which the little diamond crystals completely graphitized. Up to this threshold temperature the diamonds showed no trace of graphitization. The experimental data are shown in Fig. 19 as inverted triangles and open circles; the triangles indicate complete graphitization and the circles mean no reaction. By analogy with the direct graphite to diamond transformation<sup>11</sup> the flash-heat diamond graphitization line would be expected to be parallel to the diamond melting line but a few hundred degrees cooler. Thus, the slope of the diamond melting line just above the triple point can be inferred from that of the flash-heat diamond graphitization line.

<sup>10</sup> F. P. Bundy, H. P. Bovenkerk, H. M. Strong, and R. H. Wentorf, Jr., *J. Chem. Phys.* **35**, 383 (1961).

<sup>11</sup> F. P. Bundy, **37**, 631 (1962), following article.

<sup>12</sup> B. J. Alder and R. H. Christian, *Phys. Rev. Letters* **7**, 367 (1961).

## VII. HEAT OF FUSION OF GRAPHITE

The transient heating technique used in this investigation of graphite melting offered two ways of evaluating the heat of fusion. The first involved an analysis of the energy disposition during that part of the energy insertion period in which melting occurred. The second was based on an accounting of the heat losses during the period of solidification, identified by the "resistance dwell" in the resistance-vs-time curves (for example, Fig. 10).

In the first method the energy insertion required to attain melting temperature was determined from a series of tests such as that which served as the basis for Figs. 5 and 6. From measurements on a series of cross sections, as in Fig. 6, the fraction of graphite actually melted was determined. The energy inserted during the fusion period was consumed in three ways: first, to provide the heat of fusion; second, to provide heat and electrical losses to the walls; third, to "superheat" the center part of the column of liquid carbon to temperatures above the melting temperature.

The fraction of the graphite specimen melted, plotted as a function of total energy input, is shown in Fig. 20 for the series of samples displayed in Fig. 6. If all the additional energy inserted after melting started were used in providing heat of fusion at constant temperature this graph would be a straight line and its slope would be the heat of fusion. Lines of slopes corresponding to 10, 20, and 30 kcal/mole are drawn at the left of the chart for comparison. The fact that the line is not straight is a consequence of the losses mentioned above. However, it can be seen at a glance that the lower part of the curve is nearly straight, and its slope is a little greater than 30 kcal/mole. The detailed analysis of this set of data is presented in Table I. The consistency of the values obtained from the differ-

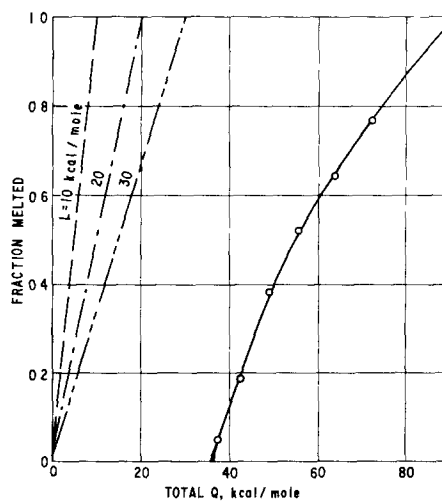


FIG. 20 Fraction of graphite melted versus total energy inserted. Measured from photomicrographs of sections shown in Fig. 6 (48 kbar series).

TABLE I. Latent heat of fusion derived from heat-up data. Spectro rod graphite, 48 kbars.  $Q_1$ , energy insertion to start of fusion, kcal/mole;  $Q_2$ , total energy insertion, kcal/mole;  $Q_w$ , wall losses, kcal/mole;  $Q_s$ , liquid superheat, kcal/mole;  $Q_F$ , heat applied to fusion, kcal/mole.

Shot volts	$Q_1$	$Q_2$	$Q_2-Q_1$	$Q_w$	$Q_s$	$Q_F$	Fraction melted	Heat of fusion
75	39.5	43.0	3.5	1.0	0	2.5	<0.18	>14
80	37.0	49.0	12.0	2.5	0	9.5	0.37	25
85	35.5	55.5	20.0	5.0	2.5	12.5	0.52	24
90	35.0	64.0	29.0	8.0	4.0	17.0	0.65	26
95	35.0	72.0	37.0	12.0	6.0	19.0	0.77	24

ent shots is remarkably good. The results indicate a value of about 25 kcal/mole.

A detailed analysis of the cool-off curves of Fig. 10 is given in Table II. The average cooling rate  $dQ/dt$  was determined from the slopes of the  $R$  versus time curves just after solidification was completed. The cooling rates vary in runs at different energy insertions because in the more energetic shots the walls were at high temperature for longer periods and hence became heated to greater depths, thus reducing the temperature gradient at the graphite-wall interface. The values of the heat of fusion obtained from the different shots in this series show more scatter than those obtained from the heat-up data. This is probably because the time intervals involved in the cool-off cases are considerably longer and less accurately defined than in the heat-up analyses. Nevertheless the resulting values average about 25 kcal/mole. It may be concluded from the total results that the heat of fusion of graphite at 48 kbar is about 25 kcal/mole, and certainly lies between 20 and 30 kcal/mole. Experimental values of the heats of fusion at other pressures have not been made. Such information would be valuable thermodynamically in the interpretation of the  $\Delta V$  upon melting by use of Clapeyron's relationship,  $L/T = \Delta V dP/dT$ .

### VIII. CONCLUSION AND DISCUSSION

Comparison of the heat of fusion obtained in the present experiments with that proposed theoretically by Pitzer and Clementi<sup>4</sup>—that is, 25 vs 10 kcal/mole—

indicates that the size of the molecules of liquid carbon must be somewhat smaller, and the degrees of freedom larger, than in the infinite polymeric chain model suggested by the theory. However, a heat of fusion of 25 kcal/mole is still quite small compared to the heat of vaporization, 175 kcal/mole. Hence only a small fraction of the graphite lattice bonds need be broken in the transformation to the liquid phase, and the molecules of the liquid phase are probably graphite-like fragments.

At pressure above 70 to 80 kbar the negative slope of the graphite melting line indicates that at the melting temperature the liquid is more dense than the solid, and becomes more so as the pressure increases. At the triple point the evidence available indicates that the diamond melting line starts off with very nearly zero slope. Thus at pressures in this range the density of liquid carbon must be about the same as diamond at melting temperature. For still higher pressures the density of the liquid must increase faster than that of diamond because the slope of the melting line of diamond gets more negative.<sup>11,12</sup>

At first thought one might suppose there would be similarities between the present type of experiment and the exploding of wires by heavy electrical discharges from capacitors. Actually there are several major differences. First, the heat-up time in the present experiments is about a thousand times slower than in most wire exploding experiments. Second, the pressures were so high that there was practically no possibility of expansion of the conductor to form a vapor, or arc,

TABLE II. Latent heat of fusion from cool-off data. Spectro rod graphite, 48 kbar.  $\Delta t$ , freezing interval, msec;  $dQ/dt$ , average cooling rate, kcal/mole msec;  $Q_1$ , total heat loss during freezing interval, kcal/mole;  $Q_s$ , liquid superheat, kcal/mole;  $Q_L$ , heat loss derived from solidification, kcal/mole.

Shot volts	$\Delta t$	$dQ/dt$	$Q_1$	$Q_s$	$Q_L$	Fraction melted	Heat of fusion
100	30	0.8	24.0	8.0	16.0	0.85	19
75	8	1.2	9.5	0	9.5	0.30	32
80	11	1.05	11.5	0	11.5	0.40	29
85	15	0.95	14.0	2.5	11.5	0.55	21
90	20	0.90	18.0	4.0	14.0	0.65	22
95	29	0.85	24.0	6.0	18.0	0.75	24

TABLE III. Thermodynamic fusion data for C, Si, and Ge

Element	$T_m$ (°K)	$\Delta H_m$ (kcal/mole)	$\Delta S_m$ (cal/mole deg)
C (graphite)	4600 (48kbar)	25	5.4
Si	1683	11	6.5
Ge	1233	8.3	6.7

phase. The current densities were far too low to produce magnetic pinch or plasma effects.

The question of the magnitude of pressure rise in the graphite rod specimens due to quick rise of temperature has been studied extensively. If one takes Bridgman's data on the compressibility of graphite to 100 kbar<sup>13</sup> and the thermal expansion data cited by Berman and Simon,<sup>14</sup> one finds that heating graphite to 4000°K at constant volume would cause a pressure rise of nearly 95 kbar. In the actual cell it was impossible for the graphite sample to be held at constant volume because it was surrounded by material of about equal modulus and density. Furthermore, it was impossible to build up any shock or dynamic pressure of appreciable magnitude because the heat-up time was of the order of a thousand times greater than the time of transit of a shock wave across the cell. Thus the pressure behavior of the cell must have been quite close to that of statically heated samples in the same kind of apparatus. A number of tests of the latter in past years<sup>10</sup> had shown the pressure rises caused by statically heating the core were less than 10%. Thus, it is believed that the transient pressure rises in the specimens in the present series of experi-

ments were less than 10% of the static background pressure.

There is considerable difference between the present experiments and those on the compression and flash sintering of graphite powders reported by Lewis, Orr, and Ubbelohde<sup>15</sup> in 1957. Their maximum pressure was about 3 kbar and the samples were loose-packed powders. They did observe permanent increases in density and decreases in electrical resistivity of their samples. They did not mention any approach to actual fusion.

It is interesting to compare the present new data on graphite with the fusion data for the neighboring elements of the same family, silicon and germanium. Table III lists the melting temperatures, heats of fusion, and entropies of fusion for these elements. While the entropy of fusion of graphite is close to those of silicon and germanium, a more fair comparison would be that of diamond because diamond has a cubic structure and tetrahedral bonding like silicon and germanium. Undoubtedly some time in the future someone will devise a way of measuring the heat of fusion of diamond.

#### ACKNOWLEDGMENTS

The author gratefully acknowledges the competent help of R. E. Tuft in carrying out the experiments, and the aid of his colleagues A. J. Nerad, H. M. Strong, P. Cannon, R. H. Wentorf, Jr., R. A. Alpher, C. Muckenfuss, and D. Turnbull in many valuable discussions of the problems and results encountered in these investigations. Special credit goes to Mrs. Theresa Brassard whose unusual skill in preparing and photographing the sections of the graphite specimens (Fig. 6) was invaluable.

<sup>13</sup> P. W. Bridgman, Proc. Am. Acad. Arts and Sci. **76**, 55 (1948).

<sup>14</sup> R. Berman and F. Simon, Z. Elektrochem. **59**, 333 (1955).

<sup>15</sup> F. A. Lewis, J. Orr, and A. R. Ubbelohde, Proc. Phys. Soc. (London) **B70**, 928 (1957).